



How to Purify and Experiment with Dye Adsorption using Carbon: Step-by-Step Procedure from Carbon Conversion from Agricultural Biomass to Concentration Measurement Using UV Vis Spectroscopy

Asep Bayu Dani Nandiyanto^{1*}, Meli Fiandini¹, Risti Ragadhita¹, Muhammad Aziz²

¹Universitas Pendidikan Indonesia, Jl Dr. Setiabudhi No 229, Bandung, Indonesia

²The University of Tokyo, Tokyo, Japan

Correspondence: E-mail: nandiyanto@upi.edu

ABSTRACT

This paper contains guidelines and provides a basic understanding of how to do experiments in dye adsorption using carbon. This paper presents a step-by-step experimental procedure from carbon preparation (as biochar) from agricultural waste to concentration measurement using UV-Vis Spectroscopy. We used agricultural waste as a model due to its high cellulose and organic content, making it easily converted into carbon. Furthermore, carbon is used as a model bioadsorbent for water treatment by the adsorption method. Here, the wastewater model used in this study is water containing organic dyes. As for the dye source model, curcumin was used in this study. This paper can be used as a guide for researchers and students in the fabrication of carbon from agricultural waste biomass easily and inexpensively for its application as an adsorbent in the batch adsorption process. This paper also supports the current issues in Sustainable Development Goals (SDGs).

ARTICLE INFO

Article History:

Submitted/Received 23 Dec 2022

First Revised 02 May 2023

Accepted 29 May 2023

First Available online 01 Jun 2023

Publication Date 01 Dec 2023

Keyword:

Adsorption,
Agricultural waste,
Biochar,
Bioadsorbent,
Carbon,
Chemistry,
Engineering,
Experiment,
Isotherm,
Particle,
Step-by-step procedure,
Sustainable development goals (SDGs),
Teaching.

1. INTRODUCTION

Pollutants in our environment by inorganic compounds (such as heavy metals) or organic compounds (such as dyestuffs), particularly in water, have become a serious human health issue that necessitates the development of strategies to reduce their amount (Abbar *et al.*, 2017). Pollutants are produced by human activity that it is not only directly harms humans and the environment, but also create secondary pollutants and harm the ecological balance indirectly (Zhang *et al.*, 2021).

Therefore, promoting clean water to restore the environment and maintain ecological balance is a formidable challenge and an urgent task. Several materials such as zero-valent iron, activated carbon, carbon nanotubes, graphene, and others have been reported for decades as adsorbent materials for water purification through adsorption and catalytic processes (Fang *et al.*, 2021). The existence of issues in water pollution needs strategies on how to solve and also how to educate people regarding this matter. Indeed, this is in line with current issues in the sustainable development goals (SDGs).

For this reason, this paper contains experimental guidelines on how to purify and experiment in water treatment. This study used the concept of dye adsorption using carbon as a model, which can be used and tried even for educational purposes. We demonstrated a step-by-step experimental procedure from carbon conversion from agricultural biomass to concentration measurement using UV-vis spectroscopy. This paper is also intended to be useful for researchers and novice students who study simple carbon preparation and adsorption experiments.

2. BASIC CONCEPT: CONVERTING CARBON FROM AGRICULTURAL WASTE FOR ADSORBENT

As a cheap and environmentally friendly type of adsorbent material for the water treatment process, agricultural waste-based adsorbents have attracted a lot of attention. This agricultural waste-based adsorbent material is usually referred to as a bioadsorbent. The use of this bioadsorbent is carried out to support current issues in SDGs.

The development of materials renewable materials must be implemented. One type of bioadsorbent from agricultural waste that is often used in water treatment is carbon. Most of the carbon is converted from agricultural waste because it contains a lot of cellulose, hemicellulose, and lignin which are the basic ingredients in converting carbon (Hao *et al.*, 2021). In addition, the conversion of carbon from agricultural waste is easy to manufacture, cost-effective, and sustainable (Tang *et al.*, 2021). Several studies have succeeded in converting carbon from various agricultural waste biomass used for water treatment (see **Table 1**).

Table 1 shows studies reporting the preparation, characterization, and application of carbon materials in water treatment, especially for adsorption. Adsorption is particularly suitable for water treatment processes because it requires only low-cost adsorbents with simple equipment and techniques for reducing chemical oxygen demand (COD) and biological oxygen demand (BOD) in wastewater (Nandiyanto *et al.*, 2020a). Until now, there has been less research providing an understanding of detailed step-by-step procedures for carbon conversion from agricultural waste as well as adsorption procedures.

Table 1. Converting carbon from agricultural wastes as bioadsorbent.

No	Agricultural wastes	Results	Reference
1	Pineapple waste	The size of the carbon particles affects the adsorption of curcumin dyes. Carbon particles of 125 μm were found to be the most efficient in the adsorption process.	(Nandiyanto <i>et al.</i> , 2020a)
2	Dragon fruit	Multilayered adsorption processes occur at all particle carbon sizes in the micrometer range, and they involve physical interactions between the adsorbate and the adsorbent surface.	(Nandiyanto <i>et al.</i> , 2020b)
3	Rice husk	Carbon derived from rice husks has a size of about 800 nm. The prepared carbon follows the Freundlich model with multilayer and heterogeneous surfaces.	(Fiandini <i>et al.</i> , 2020)
4	Pumpkin	The particle size car has a direct impact on the adsorption process. Adsorption of soursop fruit peel waste material happens on a multi-layered surface, and physical interactions occur between adsorbent adsorbate.	(Nandiyanto, 2020c)
5	Soursop	The particle size of carbon from soursop peel for the adsorption process was evaluated. Adsorption of carbon from soursop peel occurs on a layered surface with physical interaction between the adsorbent and the adsorbate.	(Nandiyanto <i>et al.</i> , 2020d)
6	Mango seed	Carbon from mango seed was evaluated for its adsorption ability. The adsorption process is suitable for the Jovanovic model. The adsorption phenomenon involves chemisorption and physisorption.	(Nandiyanto <i>et al.</i> , 2023a)
7	Jackfruit seed	Carbon from jackfruit seed waste has been successfully used in the adsorption process that occurs on monolayer surfaces, is advantageous, and is not spontaneous.	(Nandiyanto <i>et al.</i> , 2023b)
8	Papaya seed	The adsorption ability of carbon derived papaya seed was evaluated. The adsorption characteristics are compatible with the Langmuir model. The adsorption system is advantageous on monolayer surfaces with repulsive interactions.	(Ragadhita <i>et al.</i> , 2023)
9	Cassava stem	The dose of carbon-based adsorbent from cassava stems has more effect on the percentage of higher adsorption capacity. The characteristics of the adsorption isotherm show an appropriate with the Langmuir isotherm.	(Sulaiman <i>et al.</i> , 2021)
10	Walnut seed	Walnut seed-based carbon is very promising for adsorbing binary CO_2/CH_4 mixtures. Adsorption capacity values reached 0.42 and 14.03 mmol/g at optimum conditions of 1 and 10 bar, respectively.	(Bae <i>et al.</i> , 2014)

3. METHODS

To provide an understanding of how to convert carbon from agricultural waste and adsorption procedures, this paper presents a complete example of agricultural waste, namely Candlenut shell (*Aleurites moluccana*). Candlenut shell (as a precursor raw material for being converted to carbon) consists of a huge amount of cellulose, hemicellulose, and lignin, namely 28.80, 30.40, and 42.90 (w/w) %, respectively (Taslim et al., 2018). Another reason candlenut shell was chosen was that they can be found in many local markets in Bandung, Indonesia. Carbon as an adsorbent made from candlenut shell is then used in the adsorption process.

In this paper, we also used curcumin dissolved in the water as a model adsorbate solution. Curcumin was chosen as a model adsorbate because it has an ideal molecular size as an organic molecule and for safety purposes.

The equipment and materials needed in the conversion of carbon from candlenut shells to their application in the adsorption experiment are presented in **Table 2**.

In short, here, the adsorption process was carried out to remove the curcumin organic dye by being absorbed by the carbon adsorbent. To understand the adsorption process, an example concept of the

adsorption process is presented as shown in **Figure 1**.

Finally, to determine the success of processing curcumin accumulated in water, the initial and final concentrations after the adsorption process were evaluated. Not only evaluating the initial and final concentrations but also considering changes in the concentration of the curcumin solution at certain time intervals. One of the quantitative analyses that are often used to determine changes in concentration during the adsorption process, namely UV-Vis. The requirement for using UV-Vis analysis is that the sample used must be colored. If the solution to be analyzed is colorless, the sample must be stained first. The working principle of UV-Vis analysis is to compare the intensity of the light passing through the sample solution in the cuvette with the intensity of the light before it passes through the sample. The results of the UV-Vis analysis are in the form of absorbance values determined from the highest absorbance wavelength. The absorbance value is directly proportional to the concentration, that is, the greater concentration used correlates to the greater absorbance value. A more complete description of the UV-Vis spectrophotometer analysis can be seen in our previous research (Pratiwi & Nandiyanto, 2021).

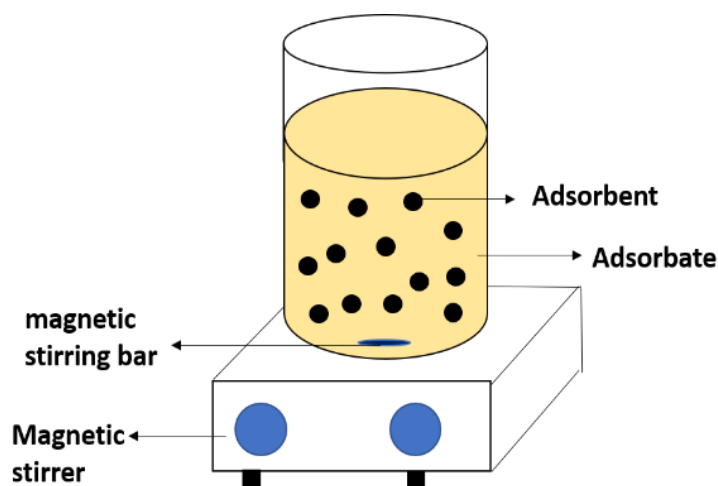


Figure 1. Adsorption toolset.

Table 2. The Example of Equipment and Materials Used.

No	Equipment	Specification	Quantity
1	Furnace	9 L	1 set
2	Beaker glass	400 mL	8 pcs
3	Magnetic stirrer	1100 rpm	5 sets
4	Measuring cup	15 mL	75 pcs
5	Sieve shaker	100 mL	1 pcs
6	Plastic cup	10, 18, 34, 60, and 120 mesh	1 set
7	Glass funnel	Diameter 60 mm	2 dozen
8	Magnetic stirrer	10 cm	3 pcs
9	Stainless steel spoon lab	25 x 7 mm	2 pcs
11	Magnetic bar	25 x 7 mm	12 pcs
10	Plastic pipette	10 mL	12 pcs
12	Analytical balance	250 g (0.001 g)	1 set
13	Mortar and pestle	16 cm	1 set
14	Microscope digital USB	1000x magnification	1 set
15	UV-Vis Spectrophotometers	Wavelength 190-1100 nm (Bandwidth 2 nm)	1 set
16	Distilled water	-	5 Liter
17	Curcumin Powder	-	5 g
18	Candlenut shell	-	1 kg
19	Zip lock plastic	14 x 17 cm	100 pcs
20	Tissue	-	1 pcs (560 sheets)
21	Aluminum foil	-	1 pcs
22	Weighing paper	-	1 set (500 pcs)
22	Filter Paper	-	1 set (12 pcs)

4. RESULTS AND DISCUSSION

The experiment was carried out in eight stages, including: (i) pre-treatment, (ii) carbonization process, (iii) and screening process, (iv) carbon characterization, (v) preparation of stock solutions and standard series, (vi) standard curve determination, (vii) adsorption process, and (viii) determination of sample concentration. **Figures 2 (a)** and **(b)** illustrate the stages of carbon conversion from candlenut shells and adsorption experiments, respectively. In more detail, the stages are described in the following sections.

4.1. Step 1: Pre-treatment Process

The pre-treatment step has several aspects: separating the shell from the contents, washing, and drying. As much as 1

kg of candlenut was separated from its contents. After the candlenut shell was separated, the candlenut shell was washed using water and removed impurities and dust. Then, dried in the sun for 24 hours.

4.2. Step 2: Carbonization Process

The dried candlenut shell waste was then carbonized using an electric oven at a temperature of 250°C for 5 hours. From the carbonization process, as much as 30 g of carbon was obtained.

4.3. Step 3: Classifying Particle Size (Optional)

This stage is optional if we need to get a specific size of the carbon. For some cases that do not need the specific size, this step can be neglected.

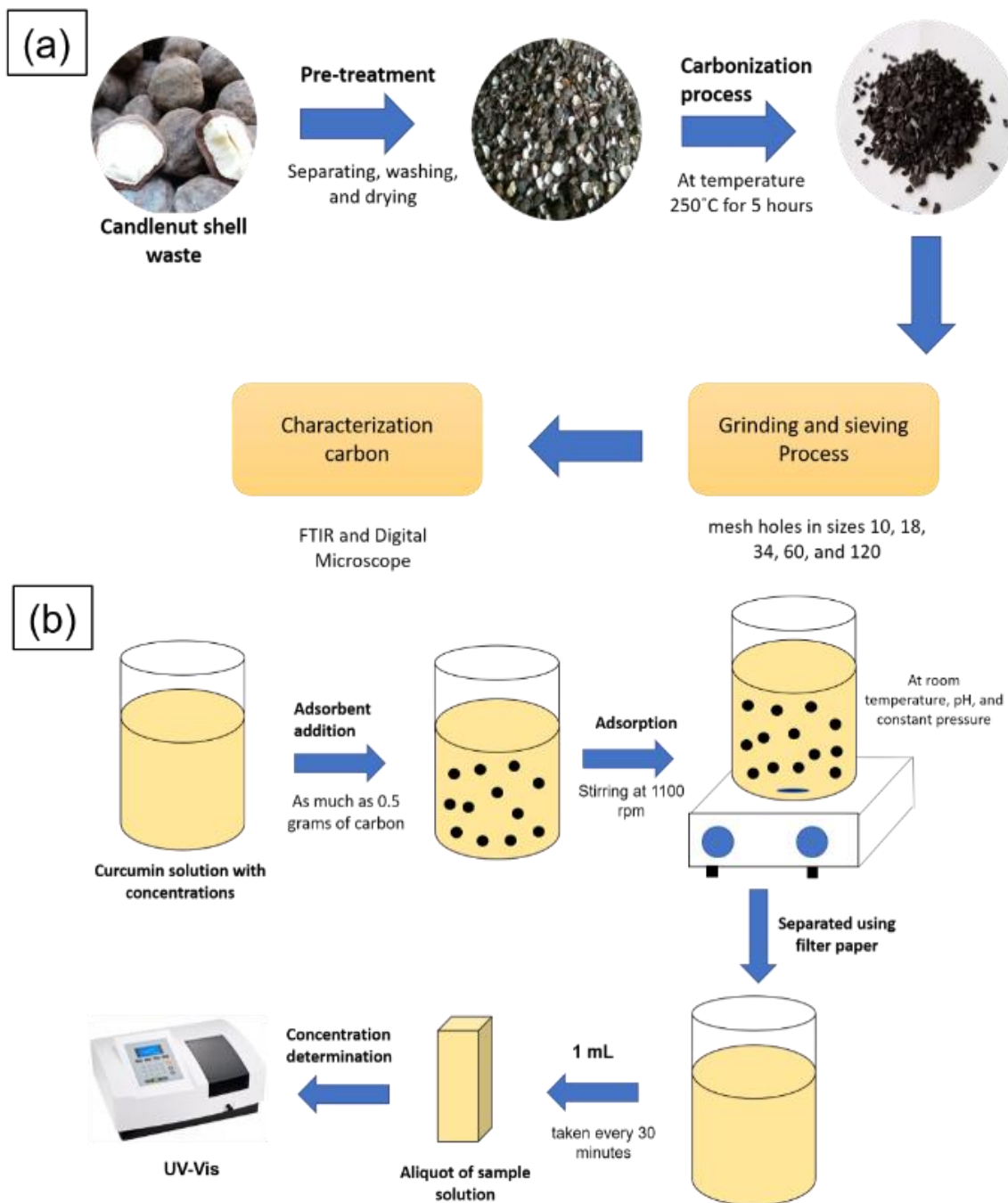


Figure 2. (a) The stages of carbon conversion from candlenut shell waste and **(b)** process adsorption steps.

At this stage, the grinding process was carried out for 3 minutes using a mortar and pestle until small carbon particles were obtained. Next, the carbon was screened using a sieve test.

The size of the mesh holes was arranged sequentially based on the largest to the smallest hole size for the distribution of carbon particles to be obtained. In this study, we used mesh with hole sizes of 10, 18, 34,

60, and 120 mesh (corresponding to 2000, 1000, 500, 250, and 125 μm , respectively). The screening was carried out in several stages as follows:

- The empty mesh (not containing carbon particles) was weighed and recorded.
- The mesh nets were arranged based on the largest to the smallest hole sizes, namely 10, 18, 34, 60, and 120 mesh.

Then, as much as 8 g of carbon was put into the largest mesh hole.

- Sieving was done by shaking. Sieving time depends on how much carbon was added to the mesh.
- After that, the carbon remaining in the mesh of various sizes was weighed and recorded. To find out the particle distribution, we calculated the mass of carbon remaining in the mesh at each size.
- Furthermore, from the mass of carbon contained in the mesh at various sizes, a curve was made to illustrate the distribution of carbon particles from candlenut shell waste as shown in **Figure 3**. Based on **Figure 3**, carbon had a size distribution in the size range of 850-1000 μm . The results of particle distribution help determine the optimal transport size to be used in adsorption.

4.4. Step 4: Carbon Particle Analysis (Optional)

This step is optional and is done to ensure the physicochemical properties of the carbon material from the carbonization. Characterization was carried out using a digital microscope (BXAW-AX-BC, China; magnification 1000x) and Fourier Transform

Infrared (FTIR, FTIR-4600, Jasco Corp., Japan) to determine surface morphology and functional groups. Actually, there are many analyzing methods, such as X-ray diffraction (Fatimah *et al.*, 2022) and electron microscope (Yolanda & Nandiyanto, 2022) to support the analysis of the material. However, this study presented simple analyses only using a digital microscope and FTIR.

Figures 4 (a-c) represent the morphology of the carbon surface of the candlenut shells with sizes of 2000, 1000, and 500 μm . Carbon has an inhomogeneous surface with an irregular shape. **Figure 5** shows the results of the FTIR analysis of carbon particles with sizes 2000, 1000, and 500 μm . Based on **Figure 5**, all carbon particles have almost similar wavelength characteristics. From the FTIR results, several functional groups were detected including -OH (hydroxyl) at a wavelength of 3859.69 cm^{-1} , C=O at a wavelength of 1680.78 cm^{-1} , C=C at the wavelength of 1204.2 cm^{-1} , and C-H at a wavelength 750.02 cm^{-1} (Simanjuntak *et al.*, 2020; Nandiyanto *et al.*, 2019; Nandiyanto *et al.*, 2023c). In addition, detailed information on how to read FTIR is presented in previous literature (Nandiyanto *et al.*, 2019; Nandiyanto *et al.* 2023c; Obinna, 2022; Sukanto & Rahmat, 2023).

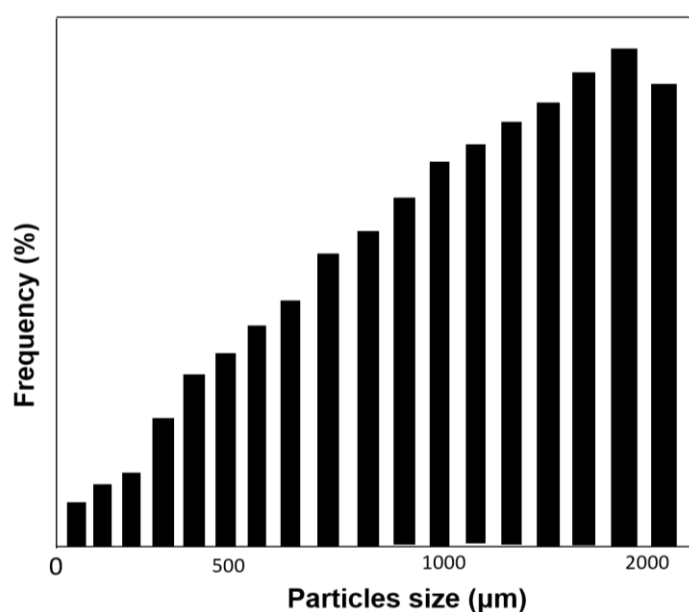


Figure 3. Distribution of carbon particles from candlenut shell.

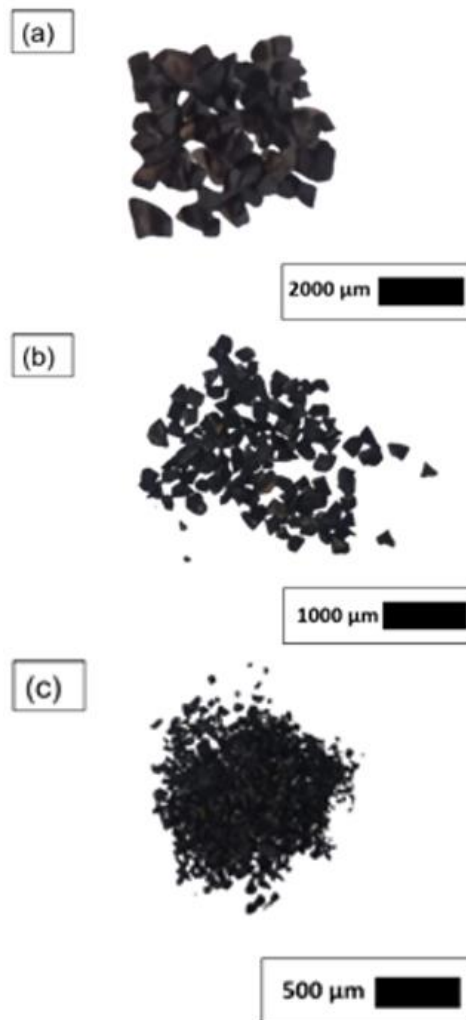


Figure 4. Microscopic images of carbon particles of various sizes (a) 2000, (b) 1000, and (c) 500 μm.

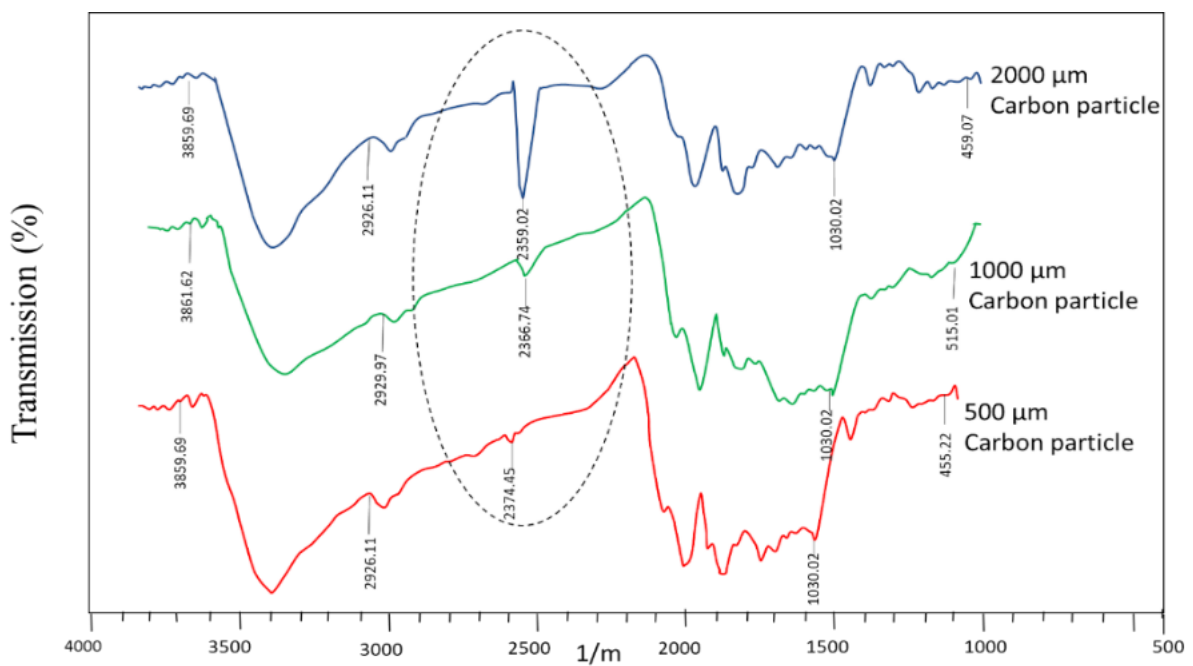


Figure 5. Results of FTIR analysis of carbon particles from candlenut shell.

4.5. Step 5: Preparation of Stock Solutions and Standard Series

Curcumin was used as a model organic dye to prepare a standard solution with a concentration of 100 ppm. In the first step, 5 g of curcumin powder was dissolved in 600 mL of water and homogenized. After that, the curcumin solution was filtered through a vacuum filter to extract the insoluble curcumin residue. The filtrate obtained from the curcumin solution is a typical curcumin solution with a concentration of 100 ppm. The next stage is the preparation of standard series solutions. In this study, a stock solution concentration of 100 ppm was diluted to concentrations of 20, 40, 60, and 80 ppm. Dilution of the solution was carried out using a dilution equation. An example of preparation of a standard series solution with a concentration of 20 ppm from a stock solution of 100 ppm with dilution is as follows:

$$V_1M_1 = V_2M_2$$

$$V_1100 \text{ ppm} = 300 \times 20$$

$$V_1 = 60 \text{ mL}$$

Thus, the standard solution of 100 ppm curcumin must be taken as 60 mL to produce a series of standard solutions with a concentration of 20 ppm in a volume of 300 mL. Furthermore, the same dilution method was adopted for the preparation of standard series adsorbate solutions with concentrations of 40, 60, and 80 ppm. Therefore, to prepare standard series adsorbate solutions with concentrations of 40, 60, and 80 ppm by taking 120, 180, and 240 mL of a standard stock solution of 100 ppm curcumin, respectively.

4.6. Step 6: Determination of a Standard Curve

Detailed information on this step is explained in our previous study regarding "How to calculate and measure solution concentration using UV-vis spectrum analysis: Supporting measurement in the chemical decomposition, photocatalysis,

phytoremediation, and adsorption process" (Nandiyanto *et al.*, 2023d).

Before determining the standard curve, several steps must be done, namely:

- The first step was to determine the maximum UV-Vis wavelength for the curcumin solution. The wavelength setting was adjusted to the complementary color of the curcumin solution. The complementary color of the curcumin solution was yellow to orange. Thus, the color absorbed was purple to blue. Therefore, we determined the maximum wavelength of curcumin to be in the range of 390–495 nm. **Figure 6** depicts the adsorption results of the curcumin solution from the wavelength scan. Based on **Figure 6**, the maximum wavelength of the curcumin solution is 395 nm because, at the 395 nm wavelength point, it shows a higher absorbance value. Since the wavelength is known, the absorbance measurement for the standard curve and the determination of the sample concentration was measured at the maximum wavelength of 395 nm. A more detailed discussion of how to determine the wavelength of the curcumin solution can be seen in our previous research (Nandiyanto *et al.*, 2023d).
- The next step, measuring the absorbance of the standard solution. Before measuring the absorbance of the standard series solution, the blank solution is first measured at a predetermined maximum wave. In this study, the blank solution was water, because water is the solvent used to make the analyte sample solution. After that, the water was removed from the cuvettes and 1 mL of standard series solutions (20, 40, 60, 80, and 100 ppm) were put into the cuvettes and the absorbance was measured using UV-Vis at the maximum wavelength (395 nm). The absorbance value of the standard series solution is presented in **Figure 7**.

- Determination of the absorbance value of the standard series solution can be done by looking at the absorbance value of the maximum wavelength (395 nm) from the adsorption graph in **Figure 7**. For example, from the adsorption results in **Figure 7**, the absorbance value of the 20 ppm standard series solution has an absorbance value of 0.243 which is presented at the maximum wavelength (395 nm). To determine the absorbance values of other standard series solutions (40, 60, 80, and 100 ppm) the method adopted was the same as for determining the adsorption values of 20 ppm standard series solutions. Furthermore, the determination of the absorbance value was recorded and tabulated in **Table 3**.
- After the adsorption data of the standard series solutions were tabulated as shown in **Table 3**, a calibration curve is prepared to obtain a linear regression equation. Based on **Table 3**, if the absorbance data is converted into a calibration curve, then a calibration curve as shown in **Figure 8** was obtained. The preparation of the calibration curve using the standard series solution method is described in detail in our previous study (Nandiyanto et al., 2023d). Based on **Figure 8**, the linear regression equation for the calibration curve is $y = 0.0094x + 0.0472$ with a correlation coefficient (R^2) = 0.9993.

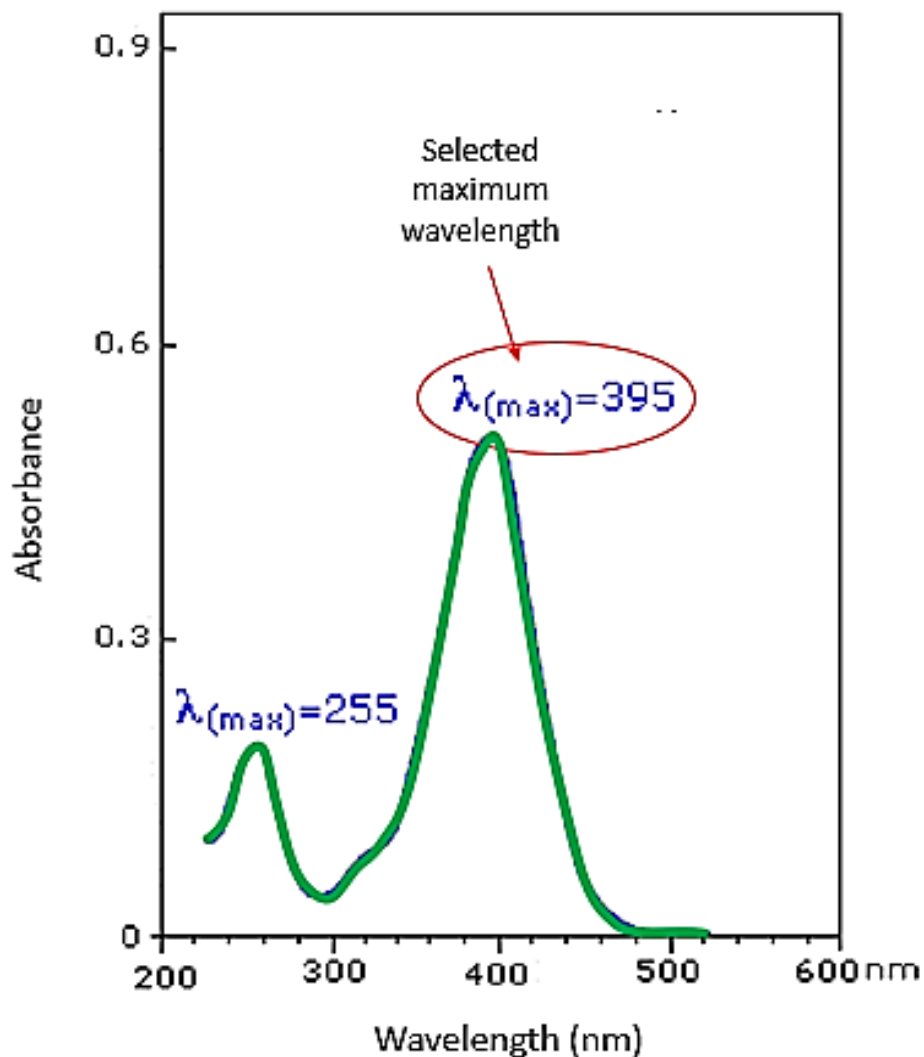


Figure 6. Example of the adsorption peak results wavelength of the curcumin solution (adsorbate). The figure was adopted from Nandiyanto et al., 2023d.

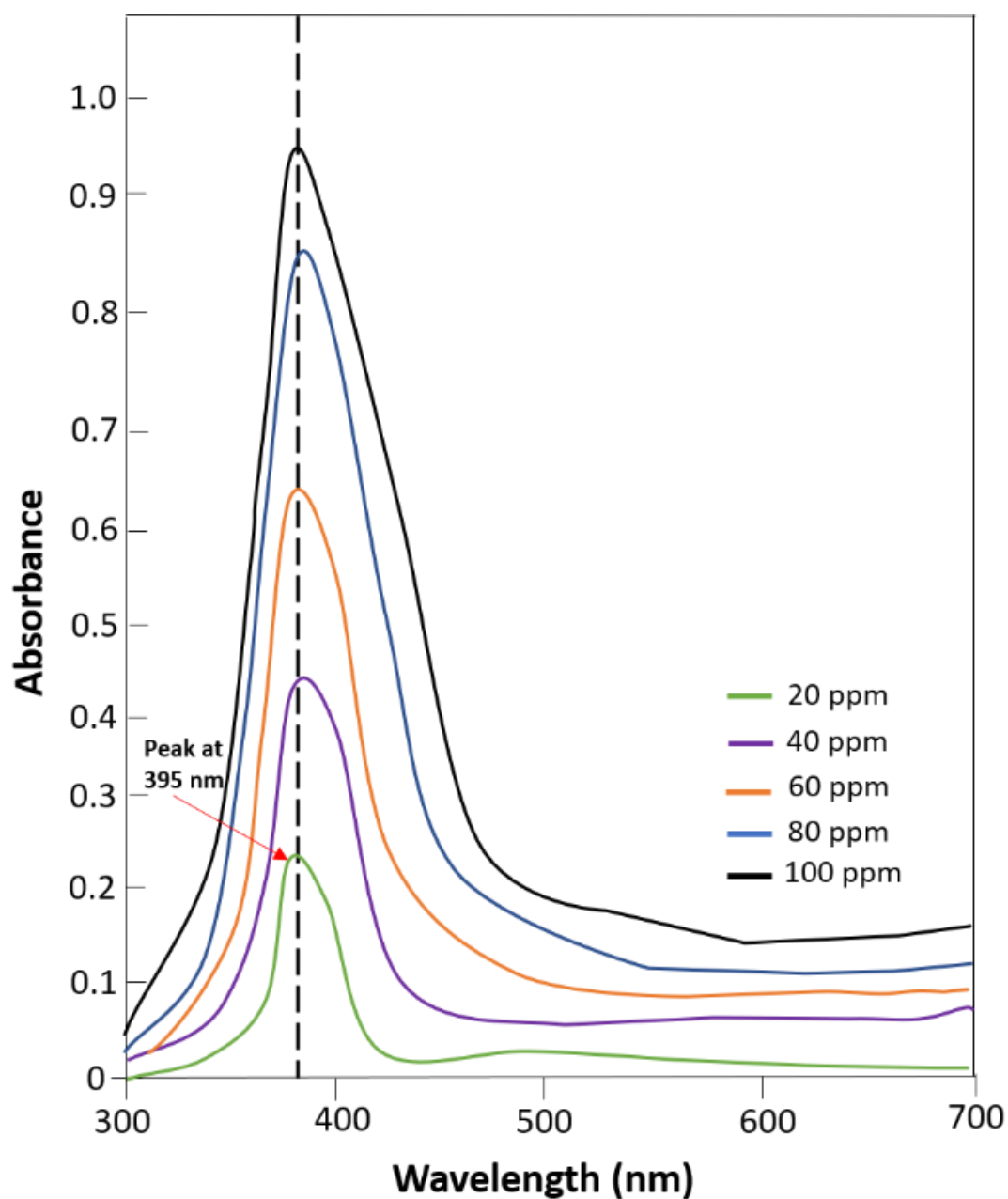


Figure 7. The UV-vis results of standard series curcumin solutions.

Table 3. Absorbance and concentration data of series curcumin standard solutions.

Concentration (ppm)	Absorbance
20	0.243
40	0.458
60	0.683
80	0.878
100	0.951

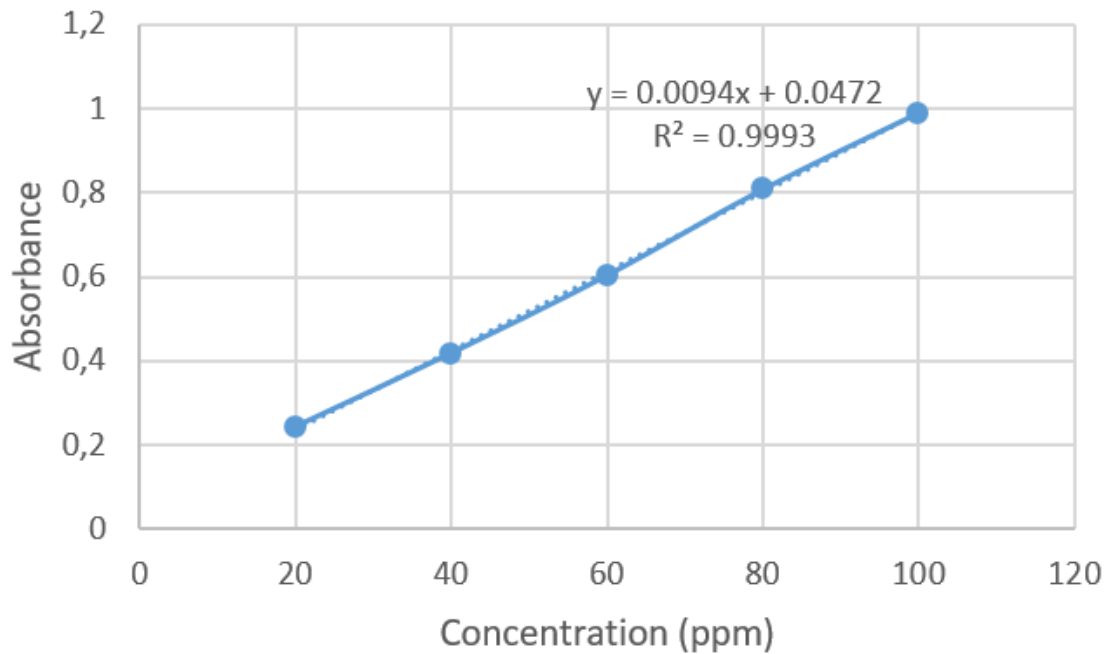


Figure 8. Calibration curve.

4.7. Step 7: Adsorption Process

Here, carbon particle sizes of 2000, 1000, and 500 μm were used as adsorbents. The purpose of using variations in the size of the adsorbent particles is to find out whether there is an effect of the particle size of the adsorbent on the adsorption results. For example, the adsorption process steps are described using relatively large carbon particles (2000 μm). However, the same adsorption steps can also be applied when the adsorption uses medium (1000 μm) and small (500 μm) sizes of carbon particles. The detailed steps of the adsorption process are as follows:

- The preparation of adsorbate solutions with various concentrations was carried out in step 5. Standard series solutions with various concentrations (i.e. 20, 40, 60, 80, and 100 ppm) were used in the adsorption process.
- Before the adsorption process, each variation in the concentration of the adsorbate solution was checked for its concentration with UV-Vis to obtain a real initial concentration of the adsorbate solution as was done in step 6.
- After the initial concentration of the adsorbate solution was obtained, 0.5 g of

carbon was added to each variation in the concentration of the adsorbate solution (i.e. 20, 40, 60, 80, and 100 ppm).

- After the adsorbent material was added to the adsorbate solution, the adsorbate-adsorbent mixture will react to absorb the pollutants in the water. This is an adsorption process, where the adsorption process is assumed to occur at a constant temperature, pH, and pressure at a certain time (e.g. 2 hours). Here, control at every 30-minute time interval was carried out to see the adsorption process.
- After the adsorption process is complete, the carbon was separated from the adsorbate solution
- The adsorbate solution that does not contain adsorbent is ready to be determined for its concentration.

4.8. Step 8: Determination of Sample Concentration

At this stage, the initial and final concentrations of the curcumin solution (adsorbate) were determined. The initial concentration of the curcumin solution accumulated in water was obtained from the absorbance measurement before

adsorption. Meanwhile, the final concentration of curcumin solution was obtained from the absorbance measurement after adsorption. After adsorption, it is hoped that the curcumin dye amount will decrease and disappear from the water. Therefore, to show the success of the adsorption process, it must be calculated and compared with the initial and final concentrations. If the final sample concentration is less than the initial concentration, adsorption has succeeded in removing the pollutant stored in the water. The steps for determining the concentration are as follows:

- A small amount of curcumin solution (adsorbate) both before and after adsorption was taken and put into the UV-Vis cuvette
- Then, the sample in the cuvettes was put into the UV-vis instrument to analyze its absorbance at the maximum wavelength
- After the absorbance value was obtained, the absorbance value was substituted in the linear regression equation which has been obtained when increasing the calibration curve to determine the concentration of the adsorbate sample, three of these steps have been carried out in steps 6-8.
- After the adsorption process was carried out, the absorbance results were obtained by checking various concentrations of curcumin solutions (adsorbate) using UV-Vis analysis instruments. As an example of the absorbance results of an adsorbate sample with a concentration of 100 ppm using carbon particles of 2000 μm at each time interval is presented in **Figure 9**. The absorbance value after adsorption can be determined by looking at the maximum wavelength absorbance value. For example, determining the absorbance value in the 10 minutes when using 2000 μm carbon. Based on **Figure 9**, the

absorbance value at 10 minutes is 0.951 which is seen at the maximum wavelength (395 nm). In addition, from **Figure 9** (see photograph image paneled in this Figure), there is a change in the color intensity of the curcumin solution over time.

- Furthermore, the results of determining the absorbance value after adsorption at each time interval are tabulated in **Table 4**.

- After obtaining the absorbance before and after adsorption, the calculation of the concentration of curcumin in the sample was carried out by substituting the absorbance value in the linear equation obtained in step 6. Below is a detailed calculation of the initial and final concentrations of curcumin solution:

Calculation of the initial concentration before the addition of 2000 μm carbon.

$$y = 0.0094x + 0.0472$$

$$0.951 = 0.0094x + 0.0472$$

$$x = \frac{0.951 - 0.0472}{0.0094} = 96.148 \text{ ppm}$$

thus, the initial sample concentration was 96.148 ppm.

Calculation of the initial concentration by the addition of 2000- μm carbon.

$$y = 0.0094x + 0.0472$$

$$0.653 = 0.0094x + 0.0472$$

$$x = \frac{0.653 - 0.0472}{0.0094} = 64.446 \text{ ppm}$$

thus, the initial sample concentration was 64.446 ppm.

- To determine the concentration of each time interval is also calculated in the same way as in calculating the concentration of curcumin solution (before adsorption treatment, 0 minutes) and final (after adsorption process, 120 minutes).

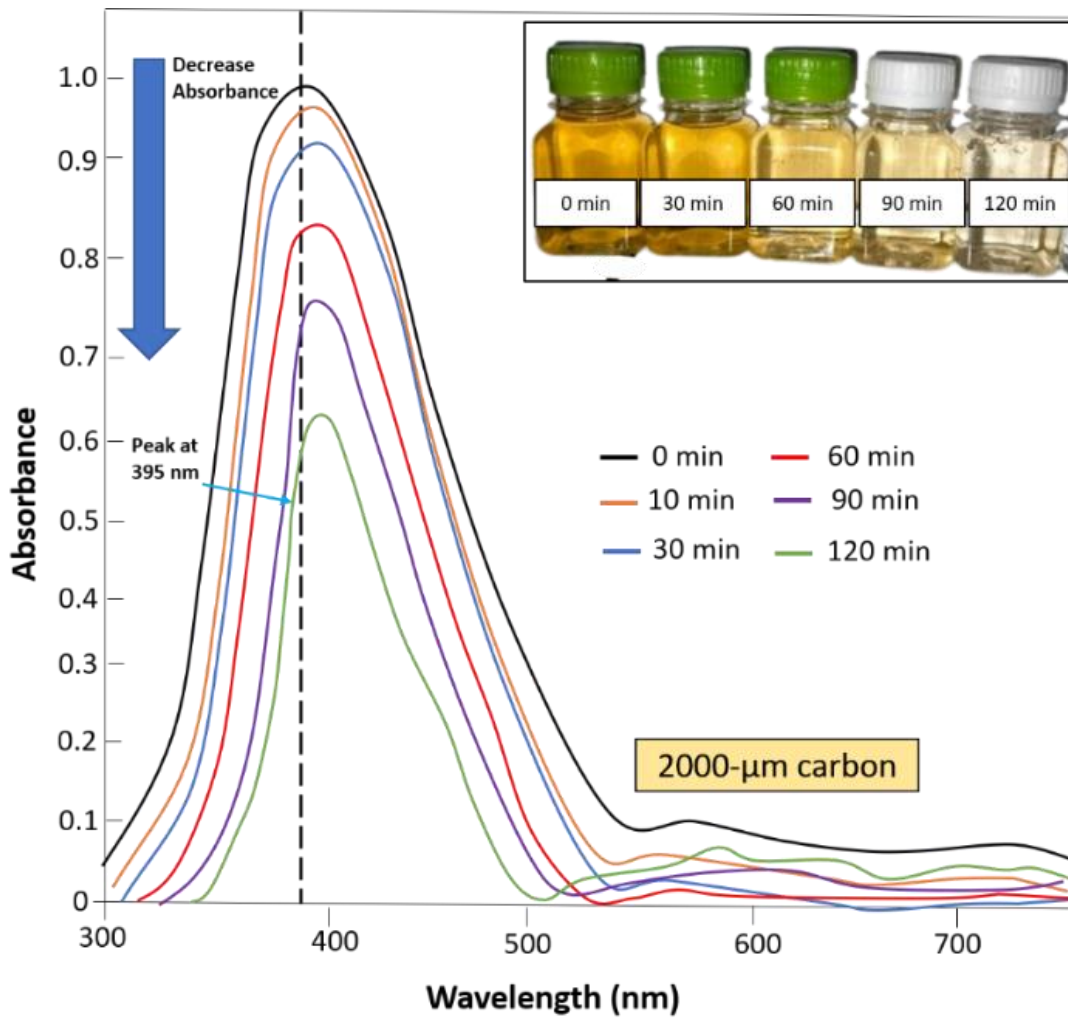


Figure 9. Absorbance of curcumin sample solution (after adsorption) with the physical appearance of the intensity of curcumin solution in an aqueous solution.

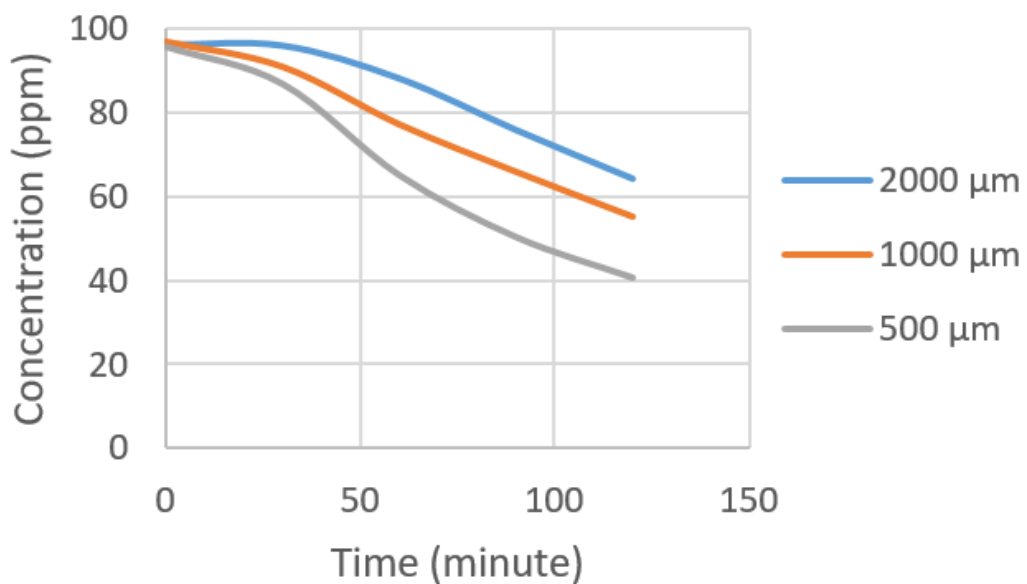


Figure 10. Decrease in the concentration of the curcumin solution at each time interval.

Table 4. Absorbance and concentration data of series curcumin standard solutions.

Carbon Particle Size (μm)	Time (minutes)	Absorbance	Calculation results Concentration (ppm)
2000	0	0.951	96.148
	10	0.950	96.042
	30	0.949	95.936
	60	0.876	88.170
	90	0.799	79.978
	120	0.653	64.446
1000	0	0.950	96.042
	10	0.949	95.936
	30	0.897	90.404
	60	0.764	76.255
	90	0.691	68.968
	120	0.567	55.290
500	0	0.949	96.489
	10	0.945	96.063
	30	0.865	87.000
	60	0.654	65.106
	90	0.543	58.268
	120	0.428	40.510

Based on **Table 4**, the initial and final concentrations of the curcumin solution that accumulated in water at each interval after the adsorption process have been identified. **Figure 10** shows the decrease in the concentration of curcumin solution at each time interval. According to **Figure 10**, the concentration of curcumin solution decreases over time after the adsorption process indicating successful adsorption.

From data **Table 4** and **Figure 10**, shows that there is an influence of carbon particles affecting adsorption ability. Smaller carbon particles have better adsorption ability than medium and large carbon particles. Because the smaller the carbon particles, the greater the surface area thus the adsorption capacity is large. Conversely, the greater the ability of the large size of carbon particles, the smaller the surface area for the adsorption capacity to be small ([Nandiyanto et al., 2023d](#)).

In addition, **Figures 9** and **10** confirm that adsorption success is characterized by reduced dye contaminants that accumulate in water after processing which is in line with

the decrease in absorbance and color intensity of the solution at each time interval.

In addition, the above data presented in **Table 4** can be used for calculating and predicting phenomena in the adsorption process. Detailed information on how to convert the data into the “adsorption phenomena” is presented in our previous study ([Ragadhita & Nandiyanto, 2021](#)).

5. CONCLUSION

This paper describes in detail the steps of carbon conversion from agricultural waste biomass and adsorption. Hopefully, this paper can be used as a basis for understanding carbon conversion from agricultural waste biomass and its application as an adsorbent in the adsorption process.

6. ACKNOWLEDGMENTS

This study awards the World Class University (WCU). Awards were also given to Bangdos, Universitas Pendidikan Indonesia.

7. AUTHORS' NOTE

of this article. The authors confirmed that the paper was free of plagiarism.

The authors declare that there is no conflict of interest regarding the publication

8. REFERENCES

- Abbar, B., Alem, A., Marcotte, S., Pantet, A., Ahfir, N. D., Bizet, L., and Duriatti, D. (2017). Experimental investigation on removal of heavy metals (Cu^{2+} , Pb^{2+} , and Zn^{2+}) from aqueous solution by flax fibres. *Process Safety and Environmental Protection*, 109(2017), 639-647.
- Bae, W., Kim, J., and Chung, J. (2014). Production of granular activated carbon from food-processing wastes (walnut shells and jujube seeds) and its adsorptive properties. *Journal of the Air and Waste Management Association*, 64(8), 879-886.
- Fang, M., Tan, X., Liu, Z., Hu, B., and Wang, X. (2021). Recent progress on metal-enhanced photocatalysis: A review on the mechanism. *Research*, 2021, 1-16.
- Fatimah, S., Ragadhita, R., Al Husaeni, D.F., and Nandiyanto, A.B.D. (2022). How to calculate crystallite size from x-ray diffraction (XRD) using scherrer method. *ASEAN Journal of Science and Engineering*, 2(1), 65-76.
- Fiandini, M., Ragadhita, R., Nandiyanto, A. B. D., and Nugraha, W. C. (2020). Adsorption characteristics of submicron porous carbon particles prepared from rice husk. *Journal Engineering Science and Technology*, 15(2020), 022-031.
- Hao, M., Qiu, M., Yang, H., Hu, B., and Wang, X. (2021). Recent advances on preparation and environmental applications of MOF-derived carbons in catalysis. *Science of the Total Environment*, 760(2021), 143333.
- Nandiyanto, A. B. D. (2020c). Isotherm adsorption of carbon microparticles prepared from pumpkin (*Cucurbita maxima*) seeds using two-parameter monolayer adsorption models and equations. *Moroccan Journal of Chemistry*, 8(3), 745-761.
- Nandiyanto, A. B. D., Al Husaeni, D. F., Ragadhita, R., Fiandini, M., Maryanti, R., and Al Husaeni, D. N. (2023a). Computational calculation of adsorption isotherm characteristics of carbon microparticles prepared from mango seed waste to support sustainable development goals (SDGs). *Journal of Engineering Science and Technology*, 18(2), 913-930.
- Nandiyanto, A. B. D., Arinalhaq, Z. F., Rahmadiani, S., Dewi, M. W., Rizky, Y. P. C., Maulidina, A., and Yunas, J. (2020d). Curcumin adsorption on carbon microparticles: Synthesis from soursop (*annonamuricata* L.) peel waste, adsorption isotherms and thermodynamic and adsorption mechanism. *International Journal of Nanoelectronics and Materials*, 13(Special issue), 173-192.
- Nandiyanto, A. B. D., Fiandini, M., Ragadhita, R., Maryanti, R., Al Husaeni, D. F., and Al Husaeni, D. N. (2023b). Removal of curcumin dyes from aqueous solutions using carbon microparticles from jackfruit seeds by batch adsorption experiment. *Journal of Engineering Science and Technology*, 18(1), 653-670.

- Nandiyanto, A. B. D., Girsang, G. C. S., Maryanti, R., Ragadhita, R., Anggraeni, S., Fauzi, F. M., and Al-Obaidi, A. S. M. (2020a). Isotherm adsorption characteristics of carbon microparticles prepared from pineapple peel waste. *Communications in Science and Technology*, 5(1), 31-39.
- Nandiyanto, A. B. D., Maryanti, R., Fiandini, M., Ragadhita, R., Usdiyana, D., Anggraeni, S., and Al-Obaidi, A. S. M. (2020b). Synthesis of carbon microparticles from red dragon fruit (*hylocereus undatus*) peel waste and their adsorption isotherm characteristics. *Molekul*, 15(3), 199-209.
- Nandiyanto, A. B. D., Oktiani, R., and Ragadhita, R. (2019). How to read and interpret FTIR spectroscopy of organic material. *Indonesian Journal of Science and Technology*, 4(1), 97-118.
- Nandiyanto, A. B. D., Ragadhita, R., and Aziz, M. (2023d) How to calculate and measure solution concentration using UV-vis spectrum analysis: Supporting measurement in the chemical decomposition, photocatalysis, phytoremediation, and adsorption process. *Indonesian Journal of Science and Technology*, 8(2), 345-362.
- Nandiyanto, A. B. D., Ragadhita, R., and Fiandini, M. (2023c). Interpretation of Fourier transform infrared spectra (FTIR): A practical approach in the polymer/plastic thermal decomposition. *Indonesian Journal of Science and Technology*, 8(1), 113-126.
- Obinna, E.N. (2022). Physicochemical properties of human hair using Fourier Transform Infra-Red (FTIR) and Scanning Electron Microscope (SEM). *ASEAN Journal for Science and Engineering in Materials*, 1(2), 71-74.
- Pratiwi, R. A., and Nandiyanto, A. B. D. (2021). How to read and interpret UV-VIS spectrophotometric results in determining the structure of chemical compounds. *Indonesian Journal of Educational Research and Technology*, 2(1), 1-20.
- Ragadhita, R., Amalliya, A., Nuryani, S., Fiandini, M., Nandiyanto, A. B. D., Hufad, A., and Al-Obaidi, A. S. M. (2023). Sustainable carbon-based biosorbent particles from papaya seed waste: preparation and adsorption isotherm. *Moroccan Journal of Chemistry*, 11(2), 395-410.
- Ragadhita, R., and Nandiyanto, A.B.D. (2021). How to calculate adsorption isotherms of particles using two-parameter monolayer adsorption models and equations. *Indonesian Journal of Science and Technology*, 6(1), 205-234.
- Simanjuntak, R., Taba, P., Baharuddin, Ibrahim, R., Murshyd, M., and Demmallino, E. B. (2020). Effectiveness of modified candlenut shell (*alleurites mollucana*) in adsorption of Fe (III) heavy metals to improve groundwater quality. *Advances in Environmental Biology*, 14(1), 36-41.
- Sukamto, S., and Rahmat, A. (2023). Evaluation of FTIR, macro and micronutrients of compost from black soldier fly residual: In context of its use as fertilizer. *ASEAN Journal of Science and Engineering*, 3(1), 21-30.
- Sulaiman, N. S., Mohamad Amini, M. H., Danish, M., Sulaiman, O., and Hashim, R. (2021). Kinetics, thermodynamics, and isotherms of methylene blue adsorption study onto cassava stem activated carbon. *Water*, 13(20), 2936.

- Tang, H., Wang, J., Zhang, S., Pang, H., Wang, X., Chen, Z. and Yu, S. (2021). Recent advances in nanoscale zero-valent iron-based materials: characteristics, environmental remediation and challenges. *Journal of Cleaner Production*, 319, 128641.
- Taslim, T., Bani, O., Iriany, I., Aryani, N., and Kaban, G. S. (2018). Preparation of activated carbon-based catalyst from candlenut shell impregnated with KOH for biodiesel production. *Key Engineering Materials*, 777, 262-267.
- Yolanda, Y.D., and Nandiyanto, A.B.D. (2022). How to read and calculate diameter size from electron microscopy images. *ASEAN Journal of Science and Engineering Education*, 2(1), 11-36.
- Zhang, S., Wang, J., Zhang, Y., Ma, J., Huang, L., Yu, S., and Wang, X. (2021). Applications of water-stable metal-organic frameworks in the removal of water pollutants: A review. *Environmental Pollution*, 291, 118076.